TURBULENCE DEVELOPMENT IN A NON-EQUILIBRIUM TURBULENT BOUNDARY LAYER WITH MILD ADVERSE PRESSURE GRADIENT

Carolyn D. Aubertine
Department of Mechanical Engineering,
Stanford University
Stanford, California 94305-3030, USA
caubertine@stanford.edu

John K. Eaton
Department of Mechanical Engineering,
Stanford University
Stanford, California 94305-3030, USA
eaton@vk.stanford.edu

ABSTRACT

High resolution laser Doppler anemometer measurements were acquired in a two-dimensional turbulent boundary layer over a four degree ramp at two momentum thickness Reynolds numbers, 3300 and 14000. The goals were to provide a detailed data set for an adverse pressure gradient boundary layer far from separation and to examine near-wall behavior of the Reynolds stresses as compared to flat plate boundary layers. The flow develops over a flat plate boundary layer before it is subjected to a varying pressure gradient along the length of the ramp and partially redevelops on a downstream flat plate. Mean velocity measurements show a log law region in all velocity profiles. Structural parameters show that there are only relatively small changes in the turbulence structure. The stresses however are perturbed by the pressure gradient with the streamwise normal stress developing an extended outer layer plateau, and the shear stress and wall-normal stress displaying outer layer peaks. Near the wall, the streamwise normal stress and shear stress collapse with flat plate data using standard scaling, but the wall normal stress is substantially larger than flat plate cases.

INTRODUCTION

Adverse pressure gradient boundary layers occur in many technologically important geometries including diffusers and the trailing edge of airfoils. Most of the previous work involving adverse pressure gradients has involved flows at or near separation, equilibrium turbulent boundary layers, as originally proposed by Clauser (1954), or flows in complex geometries. Samuel and Joubert (1974) examined an increasingly adverse pressure gradient and noted that other than the law of the wall, none of the existing models works for predicting or collapsing the data. Spalart and Watmuff (1993) compared DNS and experimental work at low Reynolds numbers, and found that the DNS produced results, which matched the experimental data, but they noted a lack of universality in their results. Tsuji and Morikawa (1976) examined a flow with alternating sign pressure gradients and found that the flow was in equilibrium for the initial adverse pressure gradient; however, as the sign of the pressure gradient alternated, the flow departed from equilibrium and did not return to an equilibrium state. Tulapurkara et al. (2001) studied an adverse pressure gradient boundary layer in a straight diffuser and noted that the turbulent kinetic energy and shear stress increase over the values for a flat plate.

Many groups have examined flows with incipient separation, near separation or just after separation. Dengel and Fernholz (1990) created an axisymmetric boundary layer with incipient separation and examined mean velocity and stress profiles for three values of the skin friction, all near zero. They found that the mean velocity profile shape is not universal since the presence of the pressure gradient causes it to change constantly. They also found that the turbulence stress levels increase throughout the flow and do not become universal or asymptotic. Alving and Fernholz (1996) examined a flow with mild separation and downstream reattachment and noted that the mean shear decreases near the wall, while increasing as it moves away from the wall. They also observed that the production and Reynolds stress peaks move to roughly the middle of the boundary layer, and the normal stress terms increase in importance as separation is approached.

Skote and Henningson (2002) performed DNS on strong adverse pressure gradient flows with and without separation and found that there are two limits, zero pressure gradient and separation, and that between these limits Reynolds number effects occur in the velocity profiles. They also noted that far from the wall, the mean velocity profiles could be collapsed using a common pressure gradient velocity scale of $u_p = (\frac{\nu}{\rho}\frac{dP}{dx})^{1/3}$.

Clauser (1954) defined an equilibrium boundary layer as one subjected to a constant force history, leading to well defined upstream history of the flow. Since the downstream development of a boundary layer depends on the upstream history of the flow as well as the local conditions, the goal of Clauser's work was to develop a flow which had a constant history and thus a well defined past. He defined a pressure gradient parameter β:

$$\beta = \frac{\delta^*}{\tau_o}\frac{dP}{dx} \tag{1}$$

where the pressure gradient is scaled by the wall shear stress, τ_o, and the displacement thickness, δ^*. When β is maintained at a constant value, the boundary layer is in equilibrium. This

requires a changing pressure gradient since the displacement thickness and wall shear change as the flow develops in the pressure gradient.

Following Clauser, many groups have examined variations on these equilibrium boundary layers. Bradshaw (1967) examined turbulent boundary layers for a wide range of values of β and found that as β increased the value of the maximum shear stress also increased. Mellor and Gibson (1966) examined the effect of the pressure gradient on the outer flow, defining a pressure velocity $u_p = \sqrt{\frac{\delta^*}{\rho}\frac{dP}{dx}}$ which they then used to define a new mean velocity defect law. Skåre and Krogstad (1994) found that equilibrium boundary layer mean profiles collapse well in both inner and outer coordinates at fixed β. They noted that β has no effect on the von Karman constant in the logarithmic law of the wall. They also observed that the turbulent stress profiles do not collapse as well in either inner or outer coordinates. Krogstad and Skåre (1995) examined an equilibrium boundary layer subjected to a strong adverse pressure gradient and found that the turbulent kinetic energy develops a second peak about halfway through the boundary layer, which affects the dissipation and diffusion rates in the outer layer. They also noted that strong anisotropy was dominant only close to the wall based on their quadrant analysis work. Krogstad and Kaspersen (2002) also examined the turbulent kinetic energy and the peaks in the production term. They noted that the outer peak moved towards the center of the boundary layer with increasing pressure gradient.

Some groups have proposed new scalings to collapse adverse pressure gradient data for a variety of different flows. Elsberry et al. (2000) studied an equilibrium boundary layer on the verge of separation and found that the flow was highly anisotropic. They noted that the turbulence was not in equilibrium with the mean flow and when scaled on the freestream velocity the stresses were seen to increase with downstream distance. They also noted that the Reynolds stress correlation has a different value than in flat plate flows and does not remain constant as the downstream distance increases. They found it was possible to collapse the correlation using a new scaling $\frac{\overline{u'v'}}{\sqrt{\overline{u'^2}\overline{v'^2}}}\frac{U_e}{U_o}$. The value for U_0 is the maximum value of the freestream velocity in the entire flow. The scaled correlation collapsed when plotted against a new length scale, $\frac{y}{\theta Re_\theta{}^{0.2}}$. The turbulent stresses were shown to collapse with the same length scale when scaled on U_0^2 for the streamwise and wall normal stresses and U_0U_e for the Reynolds shear stress. Bernard et al. (2003) examined half an airfoil and observed that the law of the wall was faithfully followed. They determined a length scale that allows the linear inner wake to tend toward a universal profile.

Perry et al. (2002) developed a closure scheme for adverse pressure gradient boundary layers. Using this scheme they found that once the mean flow evolution is correctly captured, the turbulence quantities could be determined using the work of Perry and Marusic (1995). Perry and Schofield (1973) developed a velocity defect law for adverse pressure gradient boundary layers based on the Reynolds stress profile.

The DeGraaff and Eaton (2000) mixed scaling has been observed to collapse the Reynolds stress profiles over a wide range of Reynolds numbers in the flat plate boundary layer. The wall normal stress and the Reynolds shear stress use the standard normalization $\overline{v'^2}/{U_\tau}^2$, $\overline{u'v'}/{U_\tau}^2$, while the streamwise normal stress collapse when normalized as $\overline{u'^2}/U_\tau U_e$. Recent analytical work by Marusic and Kunkel (2003) has helped to explain the reason for this scaling. However, for more complex flows, such as those subject to pressure gradients, no scaling has been found that collapses all the turbulence stress data onto simple profiles.

DeGraaff and Eaton (1999) and Song and Eaton (2004) investigated complex boundary layers subjected to strong pressure gradients, separation, and reattachment. They allowed the perturbed boundary layer to relax back towards equilibrium on a flat plate in each of these experiments and found that a stress equilibrium layer began to form adjacent to the wall as soon as the pressure gradient dropped to zero. Within the growing stress equilibrium layer, the normalized stress profiles were identical to the flat plate profiles. For computational modeling this result is quite useful because wall functions can be used confidently. However, it is only applicable in zero pressure gradient flows. A similar near-wall scaling valid in non-equilibrium pressure gradient flows would be very useful.

The objective of the current experiments is to examine a relatively mild adverse pressure gradient produced by a slow linear expansion of the test section. The pressure gradient should be large enough to perturb the boundary layer from its flat plate state, but small enough to avoid separation. Stress measurements along the length of this extended region of pressure gradient can help to identify the existence of a universal scaling for such boundary layers. This paper describes the flow development and structural changes caused by the adverse pressure gradient, as well as examining previously proposed scalings to collapse the mean velocity and turbulence profiles for a moderate range of Reynolds numbers.

EXPERIMENTS

The experiments were performed in a closed loop wind tunnel, which is mounted inside a pressure vessel. The measurements were made with a two component, high-resolution laser Doppler anemometer (LDA) described by DeGraaff and Eaton (2001). The wind tunnel test section has a rectangular cross section and is 152 mm by 711 mm by 2.9 m in length. The boundary layer is tripped 150 mm downstream of a 5 : 1 contraction and develops over a 1.5 m long flat plate. The flow is then mildly contracted over a streamwise distance of 169 mm on the bottom wall, reducing the test section height from 152 mm to 131 mm. The boundary layer then relaxes to equilibrium characteristics on a 480 mm long flat plate. At a typical freestream velocity of 15 m/s, the freestream turbulence level is approximately 0.2%.

The current flow geometry (Figure 1) consists of part of the 480 mm flat plate and a 4 degree linear expansion. The ramp expands the tunnel height from 131 mm to 152 mm. The flow does not separate along this ramp. The trailing edge of the ramp produced a small step in height between the ramp surface and the bottom surface of the wind tunnel. This step was patched using spackling and was sanded smooth. Due to this non-ideal flow surface at the trailing edge of the ramp, the flow is perturbed by surface curvature, which is not well defined. The data gathered at this location are not included in the plots of turbulence measurements that follow owing to this non-ideal surface.

The custom LDA has a measurement volume 35 μm in diameter and 60 μm in length. Due to its small measurement volume, two of the major uncertainty sources - velocity gradient bias and two-component coincidence are eliminated. The

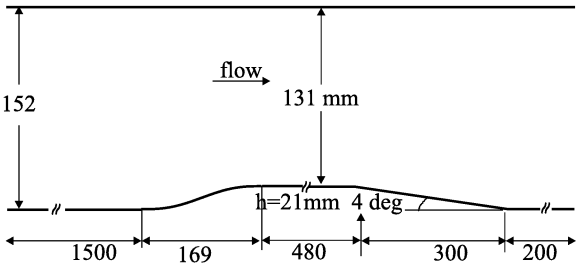

Figure 1: Current Flow Geometry

details, including the LDA bias correction, are found in DeGraaff and Eaton (2001). For 5000 samples, the uncertainties for U, $\overline{u'u'}$, $\overline{v'v'}$, $\overline{u'v'}$ are estimated as ±1.5%, ±4%, ±8% and ±10% of their local value in the center of the profiles. The average data rate is approximately 25 Hz in the freestream and considerably lower near the wall for the one atmosphere data and 5 Hz in the freestream for the four atmosphere case. Since the local values approach zero in the freestream and near the wall, the relative uncertainties in those regions are larger.

The data reported here were acquired at a nominal freestream velocity of 20.5 m/s and either one or four atmospheres of ambient pressure. The data were all gathered along the centerline of the wind tunnel in a fixed coordinate system with the x direction along the tunnel and the y direction normal to the flat plate wall. The mean and turbulent stress data taken over the ramp were then rotated by four degrees to make them perpendicular to the wall for the purpose of analysis and scaling. The values for y used in all plots are in the rotated frame and can be taken as perpendicular to the bottom surface of the flow field at all locations.

The x-axis locations, x', are the physical locations normalized by the length of the four degree ramp. This non-dimensionalization is used for all locations with the location $x' = 0.00$ being located at the leading edge of the ramp and $x' = 1.00$ representing the trailing edge of the ramp. The upstream flat plate location is therefore located at $x' = -0.33$ in this non-dimensionalization. The reference location is a flat plate boundary layer, where the mean and turbulence profiles gathered were compared with prior flat plate data to ensure that the reference location produced typical flat plate behavior.

Wall static pressure data were measured through 0.64 mm diameter surface pressure taps using a Setra differential pressure transducer (model 264). This pressure distribution gives a varying value of β , the Clauser pressure gradient parameter, ranging from 0 on the flat plate, to -1 in the mild favorable pressure gradient before the start of the ramp and to a maximum value of 2.5 along the ramp. The value of β does not remain constant along the length of the ramp, but at all locations it is relatively small, indicating that this is a mild adverse pressure gradient. The maximum value of β observed in this flow is similar to the values from the mild adverse pressure gradient equilibrium boundary layer of Clauser, where the maximum values of β is about 2.3 (Coles and Hirst, 1969). Skåre and Krogstad (1994) found values of β greater than 20 for a flow near separation.

Skin friction measurements were made using the oil-fringe imaging method described by Monson et al. (1993) for all locations except for the two upstream flat plate regions ($x' = -0.33$ and 0.00) in which a log law fit was applied instead. This technique is non-intrusive and relates the wall shear to the thinning rate of a line of oil placed on the surface. The oil, Dow Corning 200 fluid, is placed on a surface consisting of 0.13 mm thick green acetate with the back side painted flat black, at several locations and the tunnel is started impulsively. Most of the oil flows downstream during a short transient. The remaining oil forms a thin wedge which when illuminated using green monochromatic light produces interference fringes with a uniform spacing near the leading edge of the oil film. These fringes are imaged using a Kodak high resolution camera (model DC290) when a fringe pattern is evident, typically 10 minutes. Five independent measurements at each location were performed and the fringe spacing was averaged, with a repeatability of ±2%.

The fringe spacing depends on the skin friction but also on the time history of the flow, the properties of the oil, the surface properties and the viewing angle. Because of these limitations it is very difficult to estimate the absolute value of the skin friction and instead the ratio of the skin friction at the location of interest to the reference location is used. The time history, oil and surface properties are the same at both locations. For the locations along the ramp, the viewing angle for the measurement and reference locations are different and the relationship between the skin friction, C_f, and fringe spacing, ΔS_f, can be expressed as:

$$\frac{C_{f,local}}{C_{f,ref}} = \frac{\Delta S_{f,localimage}}{\Delta S_{f,refimage}} \frac{\frac{\cos\left(a\sin(\frac{\sin\theta_{light,loc}}{n_{oil}})\right)}{\cos\theta_{camera,loc}}}{\frac{\cos(a\sin(\frac{\sin\theta_{light,ref}}{n_{oil}}))}{\cos\theta_{camera,ref}}} \qquad (2)$$

where n_{oil} is the index of refraction of the oil and the angles can be computed based on the 4 degree angle of the ramp.

RESULTS

Parameters which describe the flow development at a Reynolds number of 3300, one atmosphere of ambient pressure, are given in Table 1 for the entire flow field examined. The flow development will be discussed using only the data from the one atmosphere of ambient pressure case to simplify the plots. The one and four atmosphere data will then be discussed with respect to the turbulent stresses.

Table 1: Flow parameters

x'	$U_e(m/s)$	Re_θ	$\delta_{99}(mm)$	β	*Symbol*
-0.33	20.48	3330	25.22	-0.17	●
0	20.62	2990	23.81	-0.07	■
0.25	19.87	3990	29.18	2.07	□
0.33	19.60	4210	30.41	1.74	◇
0.5	19.20	4700	33.77	1.60	△
0.67	18.80	5160	35.64	2.31	▽
0.75	18.71	5570	37.53	1.38	○
1	18.23	6680	41.76	-1.41	◆
1.33	18.26	6340	39.78	-0.37	▲
1.67	17.54	6320	38.77	-0.18	▼

The static pressure distribution, normalized by the dynamic pressure at the upstream flat plate location, $C_p = (P_{local} - P_{ref})/(0.5U^2_{ref})$, plotted against the normalized distance along the test section is shown in Figure 2. The flow

initially developed over a flat plate and then was subjected to a mild adverse pressure gradient before redeveloping along another flat plate. The pressure distribution shows that the flow encounters a short region of mild favorable pressure gradient at the top of the ramp before passing into the moderate adverse pressure gradient. At the end of the ramp, the flow starts to recover towards a zero pressure gradient, however it is still experiencing a very small favorable pressure gradient at the last measurement location.

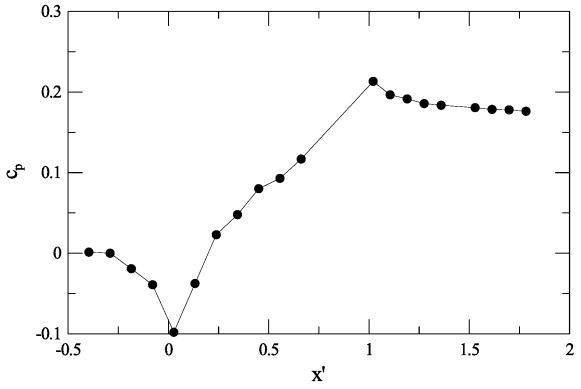

Figure 2: Pressure Distribution

The development of the skin friction coefficient, C_f, is seen in Figure 3, again plotted against the normalized distance along the test section. The skin friction coefficient can be seen to increase in the mild favorable pressure gradient before decreasing along the ramp due to the adverse pressure gradient. The boundary layer does not approach separation, but the skin friction still falls by nearly a factor of two relative to the upstream boundary layer. The freestream velocity decreases by only 11% in the same distance. Once the flow starts redeveloping along the flat plate, the skin friction coefficient again rises due to the mild favorable pressure gradient before flattening out at the last measurement location.

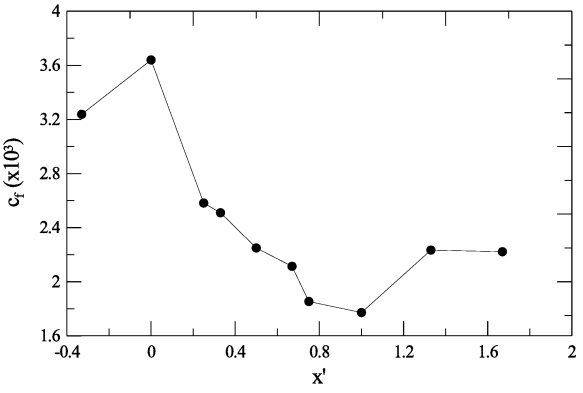

Figure 3: Skin Friction Distribution

The mean velocity data are shown in a semi-logarithmic "law of the wall" plot in Figure 4 for both the upstream flat plate and the ramp. The friction velocity used for normalization in this figure was calculated from the skin friction measured using the oil flow interferometry technique, except for the flat plate region where a traditional fit was used. The profiles all exhibit a viscous sublayer, a substantial log layer and a wake that grows as the flow proceeds down the ramp.

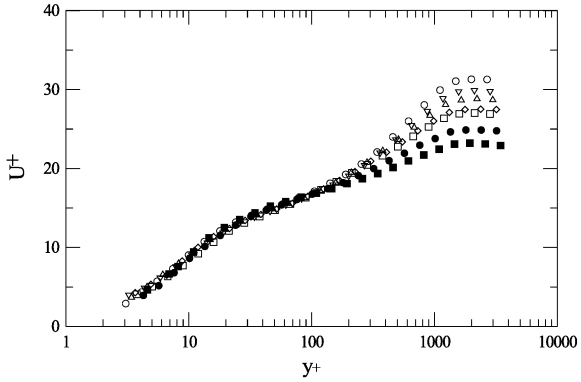

Figure 4: Law of the Wall

Figure 5 shows the development of the mean flow along the ramp. The ramp shown in this figure is drawn to scale with the vertical height expanded by a factor of two relative to the horizontal axis to show the near wall region of the flow more clearly. The flow at $x' = -0.33$ is that of a flat plate boundary layer. At the start of the ramp, the flow accelerates slightly due to the mild favorable pressure gradient caused by the curvature. The boundary layer thickens rapidly in the adverse pressure gradient, increasing by 75% along the length of the ramp. There is no inflection point observed in the flow due to the weak adverse pressure gradient. The redevelopment of the mean flow shows that the wake starts to decay, but the flow has not fully recovered to that of a flat plate by the final measurement location.

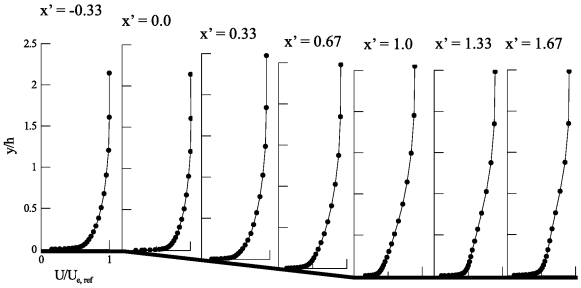

Figure 5: Mean Flow Development along ramp

The development of the streamwise and wall normal stresses are shown in Figures 6 and 7 respectively. A fixed quantity measured at the reference location was used to normalize the stresses in order to show the change in the peak stress levels as the flow develops. For the streamwise normal stress, $U_{\tau,ref}U_{e,ref}$ was used, while for the wall normal stress $U^2_{\tau,ref}$ was used (DeGraaff and Eaton 2000). The streamwise normal stress development shows that as the flow is subjected to the adverse pressure gradient, an outer plateau develops. This plateau increases in intensity relative to the inner peak as the flow progresses. The inner peak decreases as the skin friction falls. The redevelopment region shows that the plateau starts to decay and the inner peak starts to increase back towards its typical flat plate value downstream of the ramp, but the redevelopment is not complete by the final measurement station. The wall normal stress development shows the peak moving away from the wall and growing in strength as the flow travels along the ramp. In the redevelopment region, the peak starts to decay and spread out.

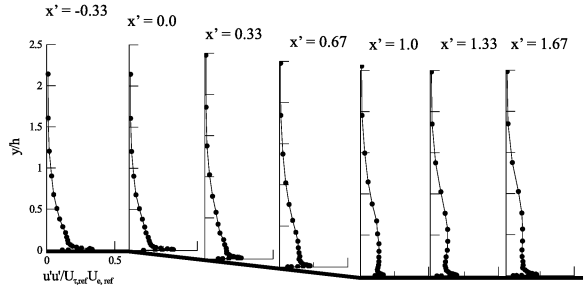

Figure 6: Streamwise Normal stress development

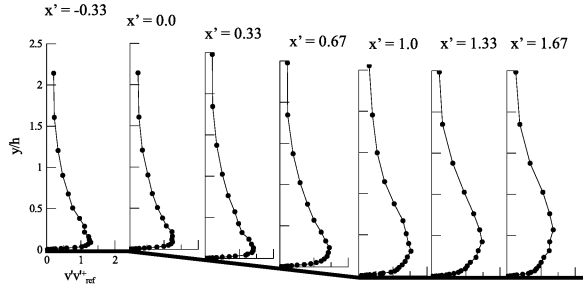

Figure 7: Wall Normal Stress Development

The development of the anisotropy parameter, $\overline{v'v'}/\overline{u'u'}$, plotted against the height above the wall scaled on the momentum thickness, is shown in Figure 8. The anisotropy parameter for the flat plate location varies between 0.3 and 0.4 throughout most of the boundary layer. As the adverse pressure gradient is imposed, the anisotropy parameter increases slightly indicating that the turbulence is becoming more isotropic. After the pressure gradient is removed, the anisotropy parameter does not recover to the zero pressure gradient value over the development length examined. The relatively small changes in the anisotropy parameter indicate that the normal stress components respond almost equally to the imposed adverse pressure gradient. This implies that there is little effect due to streamline curvature.

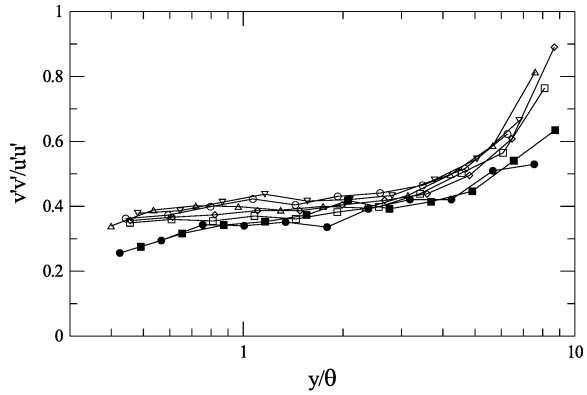

Figure 8: anisotropy

Table 2 gives the value of some important flow parameters for both the one and four atmosphere ambient pressure cases along the ramp and for the reference flat plate boundary layer.

The turbulent stress profiles for the flat plate boundary layer and a few measurement locations along the ramp are shown for both the one and four atmosphere ambient pressure

Table 2: Different Reynolds number flow parameters

$p_{amb}(atm)$	x'	$U_e(m/s)$	$\delta_{99}(mm)$	H	*Symbol*
1	-0.33	20.48	25.22	1.34	○
1	0.25	19.87	29.18	1.39	□
1	0.5	19.20	33.77	1.42	△
1	0.75	18.71	37.53	1.48	◇
4	-0.33	20.39	25.81	1.26	●
4	0.25	19.65	31.17	1.31	■
4	0.5	18.99	34.57	1.33	▲
4	0.75	18.50	36.25	1.38	◆

cases in Figures 9, 10 and 11. The Reynolds shear stress, Figure 11, shows that the traditional scaling of U_τ^2 holds for the inner region for both the flat plate and the adverse pressure gradient. However, the outer peak does not collapse in this scaling. The streamwise normal stress shows that using the DeGraaff and Eaton (2000) scaling, $U_e U_\tau$ the adverse pressure gradient data collapse in the inner layer, but do not exactly collapse on the flat plate profile. The wall normal stress is shown in Figure 10, scaled in the traditional scaling of U_τ^2, which does not collapse the increase in the peak or the movement of the peak farther out in the boundary layer.

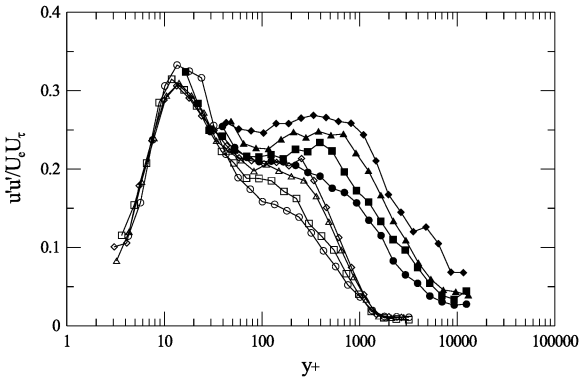

Figure 9: Streamwise Normal Stress

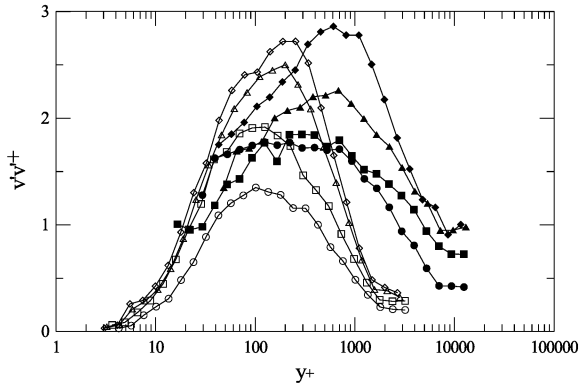

Figure 10: Wall Normal Stress

CONCLUSIONS

Experimental measurements have been presented for the flow along a four degree expansion ramp in which the Clauser

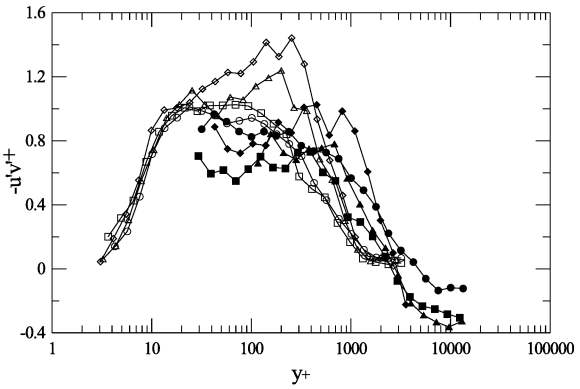

Figure 11: Reynolds Shear Stress

parameter, β, is relatively small and varies slowly. The inner layer follows the standard logarithmic law of the wall, but the extent of the log region shrinks as the wake occupies a larger fraction of the boundary layer thickness. Although the pressure gradient is mild and there is no inflection point in the mean velocity profile, the boundary layer is not in equilibrium and its shape continues to evolve. The mild adverse pressure gradient causes only small effects on the structure of the turbulence. Most non-dimensional structural parameters show only small changes as the flow enters the adverse pressure gradient region.

Profiles of the three measured Reynolds stress components are similar in the inner layer to flat plate profiles, but consistently show higher levels in the outer layer. The streamwise normal stress agrees closely with the flat plate data near the wall when plotted using the DeGraaff and Eaton (2000) mixed scaling, computed from the local skin friction and freestream velocity. However, there is a plateau of elevated normal stress in the log and wake regions of the flow. The other two stresses develop substantial peaks in the log layer that do not collapse with the flat plate data. These peaks decay when the adverse pressure gradient is removed.

ACKNOWLEDGEMENTS

We gratefully acknowledge the financial support from the Office of Naval Research contract N00014-00-10078.

REFERENCES

Alving A.E. & Fernholz, H.H., 1996, "Turbulence measurements around a mild separation bubble and downstream of reattachment", *JFM*, Vol. 322, pp. 297–328.

Bernard, A., Foucaut, J.M., Dupont, P., & Stanislas, M., 2003, "Decelerating boundary layer: a new scaling and mixing length model", *AIAA*, Vol. 41:2, pp. 248–255.

Bradshaw, P., 1967, "The turbulence structure of equilibrium boundary layers", *JFM*, Vol. 29, pp. 625–645.

Clauser, F.H., 1954, "Turbulent boundary layers in adverse pressure gradients", *J Aero Sci*, Vol. 21:2, pp. 91–108.

Coles, D.E. & Hirst, E.A., 1969, *Proceeding Computation of Turbulent Boundary Layers - 1968 AFOSR-IFP-Stanford Conference*, Vol. 2, pp.198.

DeGraaff, D.B. & Eaton, J.K., 1999, "Reynolds number scaling of the turbulent boundary layer on a flat plate and on swept and unswept bumps", *Tech Report TSD-118*, Stanford University.

DeGraaff, D.B. & Eaton, J.K., 2000, "Reynolds number scaling of the flat plate turbulent boundary layer", *JFM*, Vol. 422, pp. 319–346.

DeGraaff, D.B. & Eaton, J.K., 2001, "A high resolution laser Doppler anemometer: design, qualification, and uncertainty", *Exp Fluids*, Vol. 20, pp. 522–530.

Dengel, P. & Fernholz, H.H., 1990, "An experimental investigation of an incompressible turbulent boundary layer in the vicinity of separation", *JFM*, Vol. 212, pp. 615–636.

Elsberry, K., Loeffler, J., Zhou, D., & Wygnanski, I., 2000, "An experimental study of a boundary layer that is maintained on the verge of separation", *JFM*, Vol. 423, pp. 227–261.

Gillis, J.C., Johnston, J.P., 1983, "Turbulent boundary-layer flow and structure on a convex wall and its redevelopment on a flat wall", *JFM*, Vol. 135, pp. 123–153.

Krogstad, P. & Kaspersen, J., 2002, "Structure inclination angle in turbulent adverse pressure gradient boundary layer", *J Fluids Eng*, Vol. 142, pp. 1025–1033.

Krogstad, P.A. & Skåre, P.E., 1995, "Influence of a strong adverse pressure gradient on the turbulent structure in a boundary layer", *Phys Fluids*, Vol. 7:8, pp. 2014–2024.

Marusic, I. & Kunkel J.G., 2003, "Streamwise turbulence intensity formulation for flat-plate boundary layers", *Phys of Fluids*, Vol. 15:8, pp. 2461–2464.

Mellor, G.L. & Gibson, D.M., 1966, "Equilibrium turbulent boundary layers", *JFM*, Vol. 24, pp. 225–253.

Monson, D.J., Mateer, G.G., & Menter, F.R., 1993, "Boundary-layer transition and global skin friction measurement with an oil-fringe imaging technique", *SAE Tech Paper Series 932550*

Perry, A.E. & Marusic, I., 1995, "A wall-wake model for the turbulence structure of boundary layers. Part 1. Extension of the attached eddy hypothesis", *JFM*, Vol. 298, pp. 361–388.

Perry, A.E., Marusic, I., & Jones, M.B., 2002, "On the streamwise evolution of turbulent boundary layers in arbitrary pressure gradients", *JFM*, Vol. 461, pp. 61–91.

Perry, A.E. & Schofield, W.H., 1973, "Mean velocity and shear stress distributions in turbulent boundary layers", *Phys Fluids*, Vol. 16:12, pp. 2068 –2074.

Samuel, A.E. & Joubert, P.N., 1974, "A boundary layer developing in an increasingly adverse pressure gradient", *JFM*, Vol. 66, pp. 481–505.

Skåre, P.E. & Krogstad, P.A., 1994, "A turbulent equilibrium boundary layer near separation", *JFM*, Vol. 272, pp. 319–348.

Skote, M. & Henningson, D.S., 2002, "Direct numerical simulation of a separated turbulent boundary layer", *JFM*, Vol. 471, pp. 107–136.

Song, S. & Eaton, J.K., 2004, "Reynolds number effects on a turbulent boundary layer with separation, reattachment and recovery", *Exp in Fluids*, Vol. 36, pp. 246–258.

Spalart, P.R. & Watmuff, J.H., 1993, "Experimental and numerical study of a turbulent boundary layer with pressure gradients", *JFM*, Vol. 249, pp. 337–371.

Tsuji, Y. & Morikawa, Y., 1976, "Turbulent boundary layer with pressure gradient alternating in sign", *Aero Q*, Vol. 27, pp. 15–28.

Tulapurkara, E.G., Khoshnevis, A.B., & Narasimhan, J.L., 2001, "Wake-boundary layer interaction subject to convex and concave curvatures and adverse pressure gradient", *Exp in Fluids*, Vol. 31, pp. 697–707.